



INTERNATIONAL ATOMIC ENERGY AGENCY
UNITED NATIONS EDUCATIONAL, SCIENTIFIC AND CULTURAL ORGANIZATION



INTERNATIONAL CENTRE FOR THEORETICAL PHYSICS
34100 TRIESTE (ITALY) - P.O.B. 586 - MIRAMARE - STRADA COSTIERA 11 - TELEPHONES: 224281/2/3/4/5/6
CABLE: CENTRATOM - TELEX 460392-1

SMR/98 - 49

AUTUMN COURSE ON GEOMAGNETISM, THE IONOSPHERE
AND MAGNETOSPHERE

(21 September - 12 November 1982)

CASE STUDIES

S. RADICELLA

PRONARP

CAERCEM

Julian Alvarez 1218

1414 Buenos Aires

Argentina

These are preliminary lecture notes, intended only for distribution to participants.
Missing or extra copies are available from Room 230.

4. CASE STUDIES

4.1. Anomalous VHF transhorizon ionospheric propagation

It is known that at times VHF television signals are received at transhorizon distances producing serious interference in far away telecommunication services. Distances affected are between 500 and 4000 km if sporadic-E reflections are considered as a cause or up to 2000 km if the less probable sporadic-E scatter mechanism is invoked. Reflections from meteoric ionization can produce long distance strong interference but they are of short duration: one second approximately (see: CCIR Report 259-4).

It has been recognized for several years in Argentina that the lower TV channels transmissions are often interfered by transmitters on the same frequencies many hundred kilometers apart.

To investigate in detail such problem, the field strength of the audio signals of ZYB851, TV Channel 2, of Sao Paulo (23.2°S, 47.0°W at 59.75 MHz) has been recorded during one year (May 1980-April 1981) at Tucumán (26.8°S, 65.2°W). The audio transmitter power was 9 KW, the distance covered is 1875.5 km and the receiving antenna was a broad band log-periodic one with a gain of 6 dB over the dipole. The following analysis has been made on the basis of data obtained and elaborated by E.S.M.Moro (private communication) of the Estación Ionosférica Tucumán, Universidad Nacional de Tucumán, a group of the PRONARP of Argentina.

Fig. 4.1. shows the duration of all the events recorded when the field strength was above 2 $\mu\text{V/m}$ and 5 $\mu\text{V/m}$ respectively. An event is considered only if its duration is equal or greater than 2 min. From the figure it can be seen that the occurrence is quite high and well above the expected percentage between september and March, in spring, summer and early fall. Fig. 4.2 show the monthly percentage of the total time with presence of events. The maximum is reached in November with a value of 18.5% for $I > 2 \mu\text{V/m}$. The figure gives also the percentage from $I > 5 \mu\text{V/m}$ and $I > 20 \mu\text{V/m}$. Fig. 4.3 displays the average duration of the events in hours for given limits of field strength. Its larger values are reached between september and november with duration around two hours.

By inspecting Fig. 4.1 it is clearly seen that the propagation phenomenon under study is mainly a late afternoon and nighttime one. To show this fact quantitatively new percentages were obtained for the period of time from 20.00 and 06.00 UT that corresponds to 16.00 to 02.00 LT approximately (Fig.4.4). Values are now well above those shown in Fig. 4.2, reaching 43.5% in November

for signals with $I > 2 \mu\text{V/m}$.

It must be noticed that high fading was observed almost in each event, the only exception being the time of strong ionospheric disturbances.

The probability of Es reflections in the path involved were investigated using CCIR computer methods to search for the identification of the propagation process involved in this highly recurrent phenomenon. Values obtained make necessary to rule out this process. Also sporadic-E scatter cannot be able to produce such long lasting relatively strong signals. The only probable physical mechanism involved appears to be D region scatter taking into account in particular the normally high fading and the increase of signal quality observed during ionospheric disturbances.

It must be noticed that field strength values observed are such that produces noticeable interference in local television broadcast in the same channel 2, as informed by viewers in locations removed from the transmitter antenna, in the north of the Tucumán province.

4.1.1. Figure Captions

- Fig. 4.1. VHF TV signals long distance reception at Tucumán. Time duration of all the events recorded during the year of observations when the field strength was above 2 $\mu\text{V/m}$ and 5 $\mu\text{V/m}$ respectively.
- Fig. 4.2. VHF TV signals long distance reception at Tucumán. Monthly percentage of the total time with presence of events, for different field strength.
- Fig. 4.3. VHF TV signals long distance reception at Tucumán. Monthly average time duration of the events for different field strength.
- Fig. 4.4. VHF TV signals long distance reception at Tucumán. Monthly average time duration of the events for late afternoon and night (16.00-02.00LT) and different field strength.

PERIODOS CON INTENSIDAD DE CAMPO > 2.41 V/m

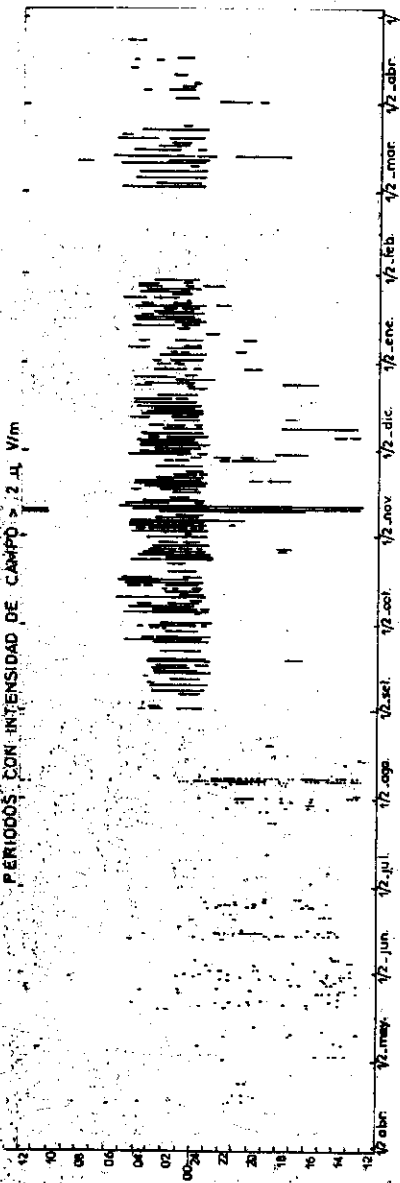


Fig. 4.1
3

PERIODOS CON INTENSIDAD DE CAMPO > 5.41 V/m

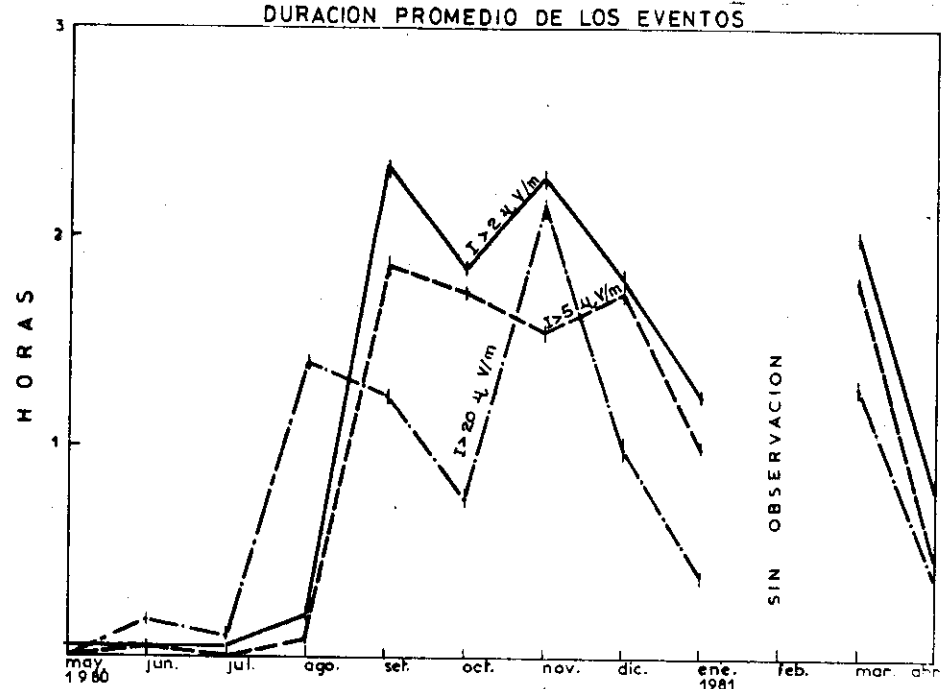
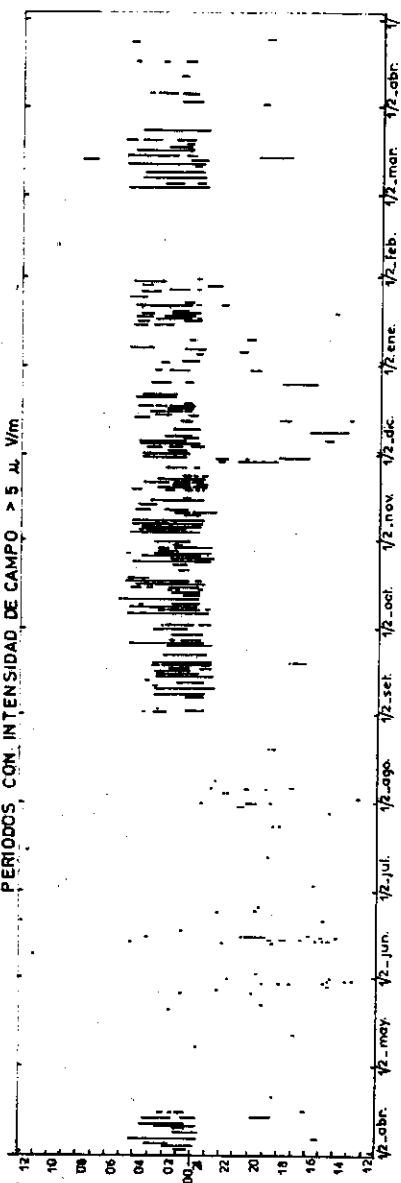


Fig. 4.2

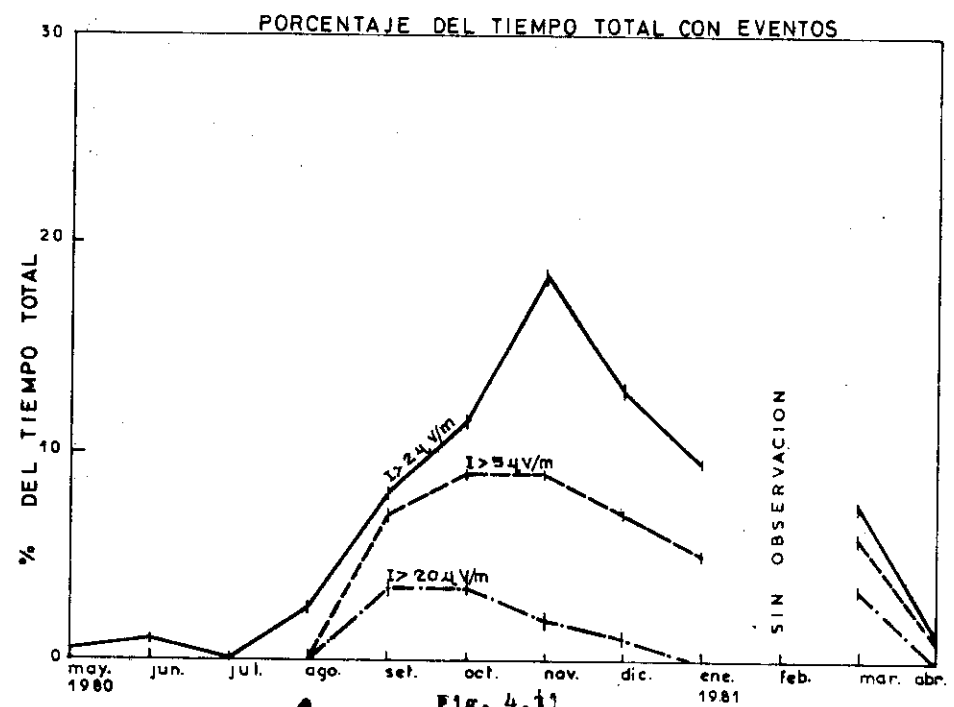


Fig. 4.3
4

PORCENTAJE DE LAS HORAS NOCTURNAS (20.00-0600 TL) CON EVENTOS

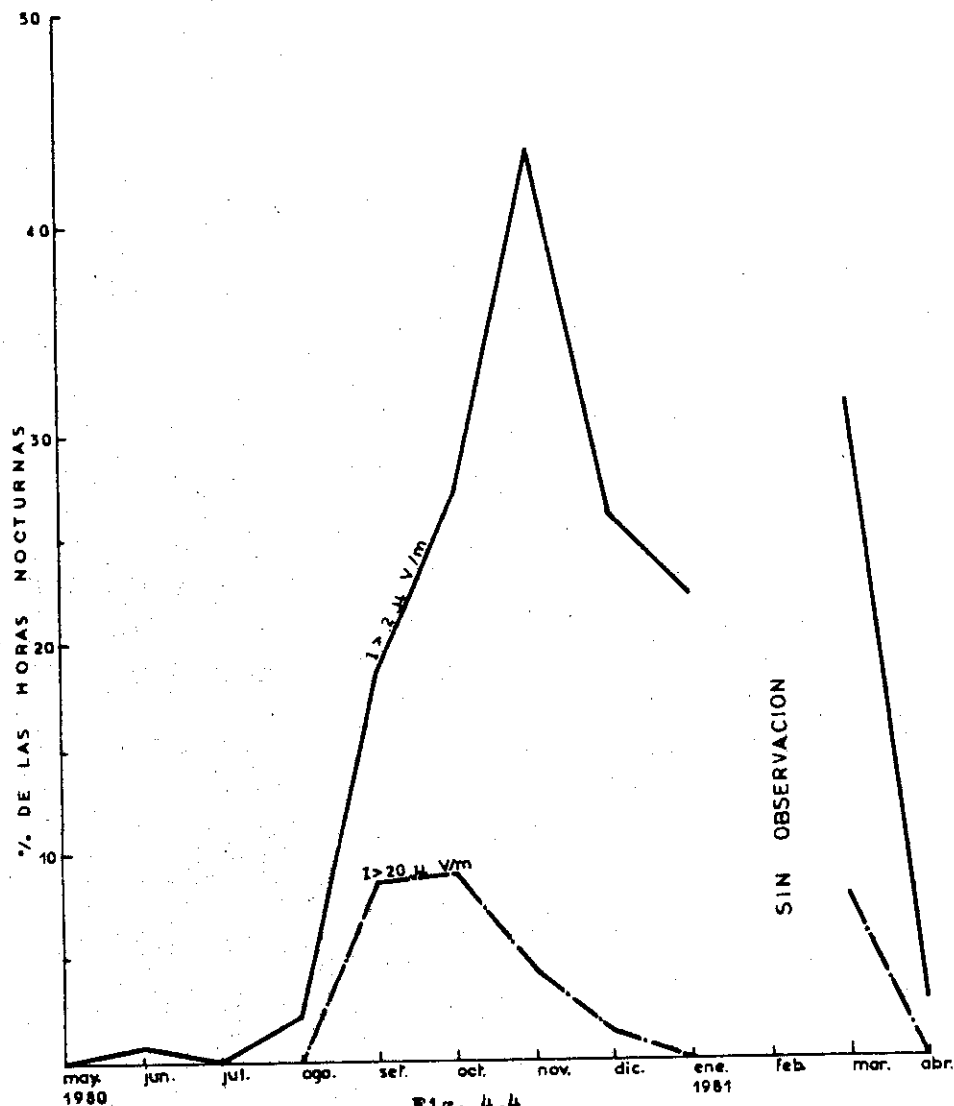


Fig. 4.4

5

4.2. Practical use of TV signal propagation over mountain-diffraction paths

4.2.1. Introduction:

The propagation of radio waves over one or more obstacles of irregular shape, gives rise to the problems of single and multiple diffraction paths, where the effects of a nonuniform transverse obstacle profile must be taken into account in field-strength predictions.

There are many difficulties when trying to calculate the diffraction loss by actual mountains or hills, because they usually cannot be seen as a single smooth diffracting obstacle, but as an irregular edged ridge.

It is, of course, impossible to derive the formula of diffraction loss for such complicated obstacles.

However, if we could assume that every diffracting mountain has a smooth surface on the top, whose radius of curvature is sufficiently large as compared with the wavelength, the problem can be treated on fairly general conditions.

The surface could be expressed as a surface of second degree having some finite radius of curvature such as a cylinder, and the attenuation coefficient, i.e. the ratio of the field strength to that in free space, can be deduced in a similar form to that corresponding to the ordinary Van der Pol and Bremmer formula for diffraction by a large spherical surface.

The results, in this case, are correct even when the transmitter and receiver are at great distances from the diffraction surface as compared with the radius of curvature.

In the extreme case where the radius of curvature tends to zero, we can associate the obstacle with a plane normal to the direction of propagation.

The case of a single "knife-edge" obstacle has been investigated in theory and practice for more than forty years. There is a general agreement on the validity of the classical approach based on the Fresnel-Kirchhoff scalar theory for optics, which expresses the diffraction loss over a sharp ridge as a function of the frequency f , the partial distances from the terminals to the obstacle and the height h from the top of the ridge to the line joining both antennas.

Though frequently encountered in the field, the case of two knife-edge obstacles or more has been only formally studied during the last two decades. A complete mathematical analysis was made by Millington (1962) involving the computation of a multiple Fresnel integral whose dimension is equal to the number of diffracting mountains. This solution is unsuitable whenever there are more than two intervening hills. For this reason, the use of empirical approximations such as those of

6

Epstein and Peterson (1953) and Deygout (1966) is preferable for most practical computation purposes. The solution suggested by Deygout gives better results than that of Epstein and Peterson when compared with Millington's analysis. However - when the diffraction loss reaches a maximum, Deygout's method becomes pessimistic and the approximate value exceeds the theoretical one by 2 to 5 dB.

Another approximation has been suggested by C.López Giovaneli (1982), ("Multiple Knife-Edge Diffraction, Comparative Analysis of Simplified Solutions", sent for publication), which gives results that agree with those of Millington in several cases.

4.2.2. Application to mountain diffraction path calculations.

Typical terrestrial diffraction paths are frequently encountered in - mountainous zones such as those of west territories in Argentina.

In many cases it is impossible to select repeater sites that are in - "line-of-sight" (LOS) of each other, due to the presence of elevated ridges along the path between terminals, where the installation of power plants necessary for the operation of communication systems as well as maintenance possibilities are impracticable.

However if the predicted field strength value after diffraction by - mountains, is above certain threshold level that ensures the necessary propagation reliability, the radiolink will meet the required performance for an adequate - - signal to noise ratio.

In order to obtain a more complete picture of a radiolink transmission via diffraction paths, we must take into account that wave energy is also reflected from flat surfaces such as water, ground or sides of metal buildings, refracted or bent by the atmosphere along the pathlength, reflected from stratified - - layers on the atmosphere or scattered by irregularities in the refractive index - or by atmospheric air turbulence.

Fading due to propagation mechanisms involves refraction, reflection, diffraction, scattering, focussing attenuation and other causes. We can distinguish between two general types of fading: multipath fading due to interference between a direct wave and a wave reflected from the ground or from atmospheric sheets or layers, and power fading or "slow fading" due to the presence of an unusually - small vertical refractivity gradient along the propagation path.

In the study of a V.H.F. television link made in San Juan (Argentina) in 1981, which is presented in section 4.2.3., we have only considered the transmission loss due to diffraction over two knife-edge obstacles under conditions of standard refraction, which is equivalent to an effective earth radius coefficient $K=1,33$.

In this link the earth-reflected wave can be neglected because the first

Fresnel-zone clearance is obtained in the foreground of each antenna and the presence of rough earth along the path contributes to the scattering of the reflected energy.

The determination of propagation reliability expressed as a percentage of time the received signal will be above a certain threshold and the fade margin under all anticipated climatic conditions, will not be included in section 4.2.3, though it is important to note that in practice, it is necessary to perform this computation to obtain a complete design of the system.

4.2.3. Study of an actual V.H.F. television link

The work described was done by C.López Giovaneli, from the Centro de Investigaciones Regionales de San Juan, integrated in the National Programme of Radiopropagation of Argentina.

The objective of this study is to compute the total transmission loss between two terminals that are not in "line-of-sight" of each other.

The point-to-point television link was designed to provide colour - - television service to remote locations that are situated in a completely shadowed area where LOS operation is impracticable. The transmitter was installed at Mogote Los Corralitos, San Juan, at an elevation of 3.162 m. above sea level. The - - receiving point is at Cerro El Dique, Valle Fertil, San Juan, 83,4 km. from the - transmitter, and at an elevation of 1.400 m. above sea level.

Between these two points there is a mountain chain where the installation of a radio relay station is impracticable.

Path profile exhibits two hills above the line joining the transmitter - and the receiver (line TR).

This is a case of double knife-edge diffraction with two "positive" - obstacles.

The problem has been treated with the aid of the approximation suggested by C.López Giovaneli (solution L) and the results have been compared with the - measured values.

Predictions made by this method shows good agreement with the measured values and a better performance in comparison with the results obtained through the use of Deygout's approximation (solution D).

The intersection of the lines joining the transmitter with the top of -

obstacles M2 (66.4 Km from the transmitter) and the receiver with the top of obstacle M1 (60.2 Km from the transmitter), point P, divides the total propagation path between T and R into two diffraction paths TM1P and PM2R. The diffraction loss associated with M1 is computed first by considering an effective height h'_1 for M1. The diffraction loss associated with the second hill M2 is then computed by considering an effective height h'_2 .

$$h'_1 = h_1 - \frac{d_1 \cdot h_2}{d_1 + d_2} \quad (1)$$

$$h'_2 = h_2 - \frac{d_3 \cdot h_1}{d_2 + d_3} \quad (2)$$

Where h_1 and h_2 are the heights from the top of M1 and M2 respectively, to the line joining T with R.

The total diffraction loss is obtained by adding the partial losses over M1 and M2.

$$am_T = am_1 + am_2 \quad (3)$$

where:

$$am_1 = f(d_1, k_1 d_2, h=h'_1) \quad (4)$$

$$am_2 = f(k_2 d_2, d_3, h=h'_2) \quad (5)$$

the coefficients k_1 and k_2 are functions of the intervening heights and distances,

$$k_1 = f_1(X_p, d_1, d_2) \quad (6)$$

$$k_2 = f_2(X_p, d_1, d_2) \quad (7)$$

$$X_p = f(h_1, h_2, d_1, d_2, d_3) \quad (8)$$

where X_p is the distance between the transmitter and point P.

The total transmission loss is:

$$a_T = a_0 + am_T \quad (9)$$

where:

$$a_0 \text{ (dB)} = 32.5 + 20 \log F \text{ (MHz)} + 20 \log d \text{ (Km)} \quad (10)$$

a_0 is the free space loss in decibels between two isotropics antennas separated by d kilometers at a frequency F in megahertz.

The computation involved in this case, was performed through the use of a programmable calculator. The television transmitter is operated on Channel 13 with 260 W of peak video transmitter power. The transmitter antenna system is a vertical array composed of five antennas of the corner reflector type with a total power gain (over a half wave dipole) of 16.5 dB. The transmitter antenna tower height is of 24m. The measurements were made with a half wave dipole (0 dB) at a height of 6m above ground. Insertion losses of connectors and power splitters are in the order of 2 dB. Near-end transmit and far-end receive transmission line losses are in the order of 0.8 dB. The insertion loss of matching pad device (balun) at the input of the field strength meter, is of 1 dB.

The following values were obtained from the path profile and through the use of geometrical formulas in a computer program, by considering standard refraction with an effective 4/3 earth radius.

$$h_1 = 181\text{m} \quad (\text{Hill M1, 2000m height, 60.2 Km from transmitter})$$

$$h_2 = 167.57\text{m} \quad (\text{Hill M2, 1870m height, 66.4 Km from transmitter})$$

$$h'_1 = 29\text{m}$$

$$h'_2 = 35\text{m}$$

For solution D it is necessary to determine the "main obstacle", that is the main individual loss or the greatest ratio h/r , where r is the radius of the first Fresnel-zone at the position of the obstacle. In our case M2 is the "main hill".

The determination of X_p , k_1 and k_2 , the parameters used in solution L, gives the following values:

$$X_p = 63.016 \text{ Km} \quad ; \quad H_p = 1924.53\text{m} \quad (\text{height of point P})$$

$$k_1 = 0.4542$$

$$k_2 = 0.5458$$

It is important to note that this method is symmetrical, that is, it is not necessary to define which is the main obstacle as in Deygout's case.

Considering a frequency $F = 213 \text{ MHz}$ and an average transmitting power of 130 W (51.14 dBm) we obtain the following values for solution L and solution D in comparison with measurements made at the reception point.

	Solution L	Solution D	Measurement
am ₁	12 dB	18,3 dB	
am ₂	13 dB	10 dB	
a ₀	117,5 dB	117,5 dB	
a _T	142,5 dB	145,8 dB	143 dB

The difference between the measured value and the prediction made with solution L is only of 0,5 dB.

For solution D the deviation is of 2,8 dB.

Solution D becomes pessimistic for short spacing of hills and when the diffraction loss reaches a maximum:

$$\frac{h_1}{r_1} \approx \frac{h_2}{r_2}$$

Conclusion

In order to obtain a signal level of 56 dBu (decibels related to 1 - microvolt) at the input of the repeater system located at the reception point (Cerro El Dique, Valle Fértil, San Juan), it will be necessary to install a Yagi array with a total power gain of 16 dB (over half wave dipole) at 36 m. above ground. The far-end receive transmission line loss must be less than 1,2 dB. The average transmitting power must be 1,6 Kw (2,04 dBk).

With 56 dBu we can obtain a fine video image with "snow" just perceptible.

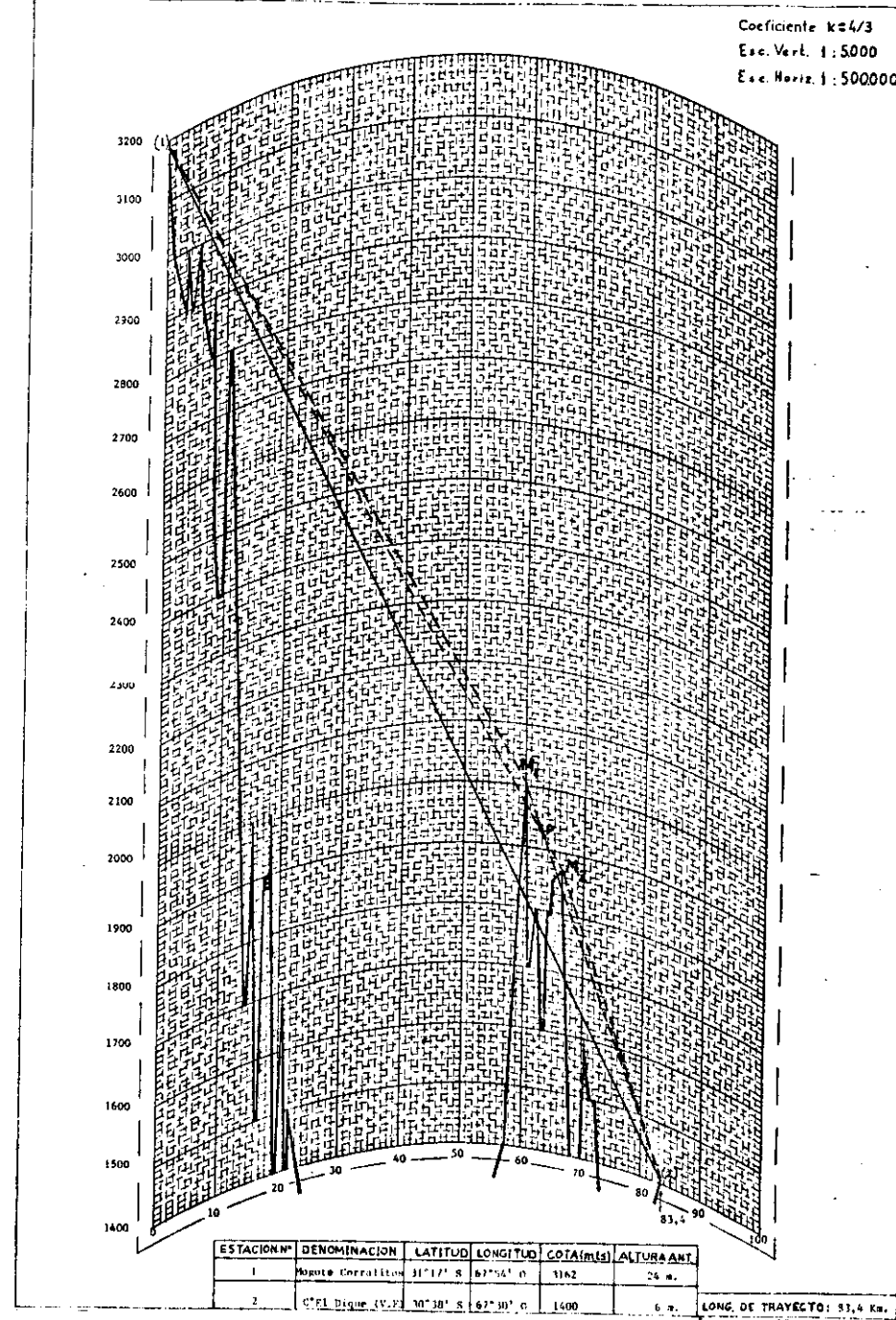
The fade margin is of about 10-15 dB for this particular link. It has been observed power or diffraction fading during sunrise with marked decrease in signal level. This slow fading persist for several hours after sunrise until it ceases around midday before transmission normally begins.

From the steady midday signal an increase of signal strength has been observed, especially 2 to 3 hours after sunset.

Since the transmitter is normally operated from 12.30 to 0.30 hr. the link is not essentially affected by fading.

An increase of average signal level can be expected at night (on calm, clear nights particularly), especially in summer when the diurnal effects are more pronounced than in winter.

11



12

Fig. 4.5

4.3.- BRAZILIAN EXPERIENCE ON

RAIN ATTENUATION (*)

This section presents some results concerning the Brazilian experience on rain attenuation at frequencies above 10 GHz. Up to now there are 3 years of data for an 8.6 km path, operating at 10.915 GHz in the urban area of Rio de Janeiro (maritime tropical climate). Two more paths have begun to be studied recently, one in mid-1980 and the other early this year. The propagation measurements for these paths will be published soon. As a complement to the experimental work, two mathematical models for terrestrial and earth-space paths were developed [11],[12].

RAIN CELL MODEL

The interpretation of rain attenuation measurements was based in the cylindrical rain cell model (Figure 4.6) proposed by Misme and Fimbel [13],[14], which dimensions are given by,

$$D(\text{km}) = 2.2 \left[\frac{100}{R} \right]^{0.4} \quad (7)$$

and

$$R_0 = 10 \text{ mm/hr (residual precipitation)}$$

According to the authors, these values seem to be independent of climate. In its definition, data from Japan, Malaysia, Switzerland and France [15] have been used. As will be seen later, the results presented here also tend to confirm this assumption.

TERRESTRIAL PATHS

As cited previously, the first experience in Brazil on rainfall attenuation measurements at frequencies above 10 GHz was carried out in the urban area of Rio de Janeiro. A commercial link owned by EMBRATEL (Brazilian Enterprise of Telecommunications) was used. The link parameters are given below:

Capacity:	2700 Telephonic Channels
Frequency:	10.915 GHz
Distance:	8.6 km
Transmitting Power:	38.5 dBm
Antenna Gain:	49.8 dB
Free Space Attenuation:	132.1 dB
Additional losses:	16.7 dB
Nominal Receiving power:	-10.7 dBm
Receiver Threshold:	-78.5 dBm
Fading Margin:	67.8 dB

Precipitation rate was measured simultaneously with rainfall attenuation. The rain gauge was a Hellmann-Fue type (5 min. integration time) located 3.2 km from one terminal as depicted in Figure 4.7. The statistical distribution of precipitation rate is shown in Figure 4.8. A constant correction of 20 mm/hr was introduced in order to adjust the difference between 5 and 1 min. integration time.

* This section taken from Pontes and Assis (1981) [see section 4.2.3]

Figure 4.9 shows the theoretical and experimental distributions of rain attenuation, corresponding to the period from 07/15/77 to 07/14/78 [16]. The theoretical calculation has used the precipitation rate data given in Figure 25 and was based in a mathematical model developed by Assis and Einloft [11]. As can be seen from Figure 26, there is a close agreement between theoretical and experimental results. The three years of data, not shown here, covering the period from 07/15/77 to 07/14/80, are also in accordance with predictions by the mathematical model [11].

The theoretical analysis has used a model which is based on the rain cell behaviour along the path, assuming a statistical independence among rain cells and also that, for a long observation period, a given precipitation rate will be exceeded during the same percentage of time at all points in the propagation path. Since the most important contribution for attenuation is given by the area of most intense precipitation (cylinder with diameter D in Figure 23), for a distance d it is possible to have in different periods of time a total of d/D rain cells. According to these ideas, if a rain cell has a diameter D which corresponds to a precipitation rate R exceeded for a time percentage P' , the attenuation produced by this cell in a distance d will be exceeded for a percentage P given by [11],

$$P = \frac{d}{D} P' \quad (8)$$

Using the geometry in Figure 23 theoretical attenuation can be easily computed by:

$$A(\text{dB}) = k [R(\text{mm/hr})]^\alpha D(\text{km}) + k[10]^\alpha [d(\text{km}) - D(\text{km})] \quad (9a)$$

for $d < 33$ km, and

$$A(\text{dB}) = k[R(\text{mm/hr})]^\alpha D(\text{km}) + k[10]^\alpha [33 - D(\text{km})] \quad (9b)$$

for $d > 33$ km, where the parameters k and α can be calculated, for instance, from Misme and Benoit-Guyot [17] or Olsen et al. [18].

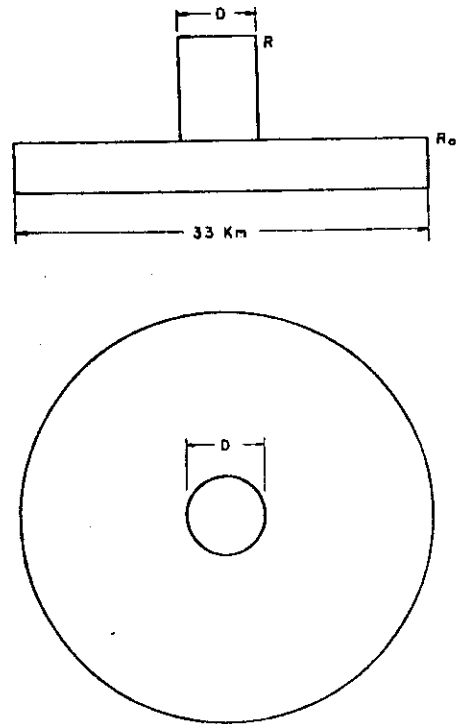


Fig. 4.6 - Cylindrical rain cell

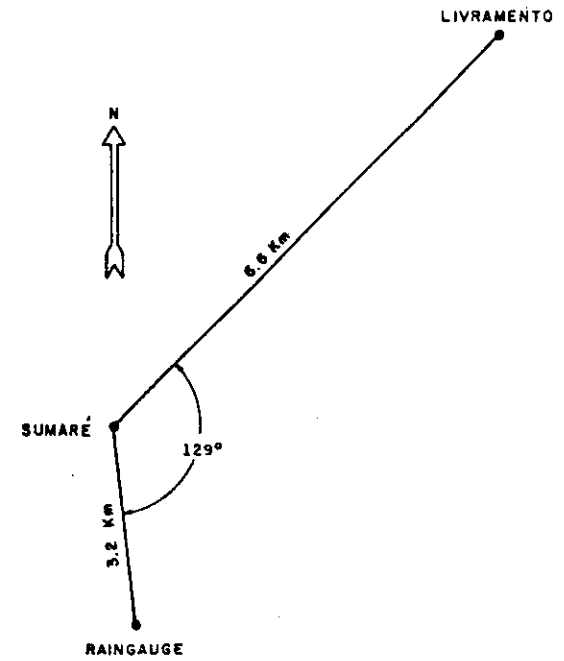


Fig. 4.7 - Raingauge location relative to radio link

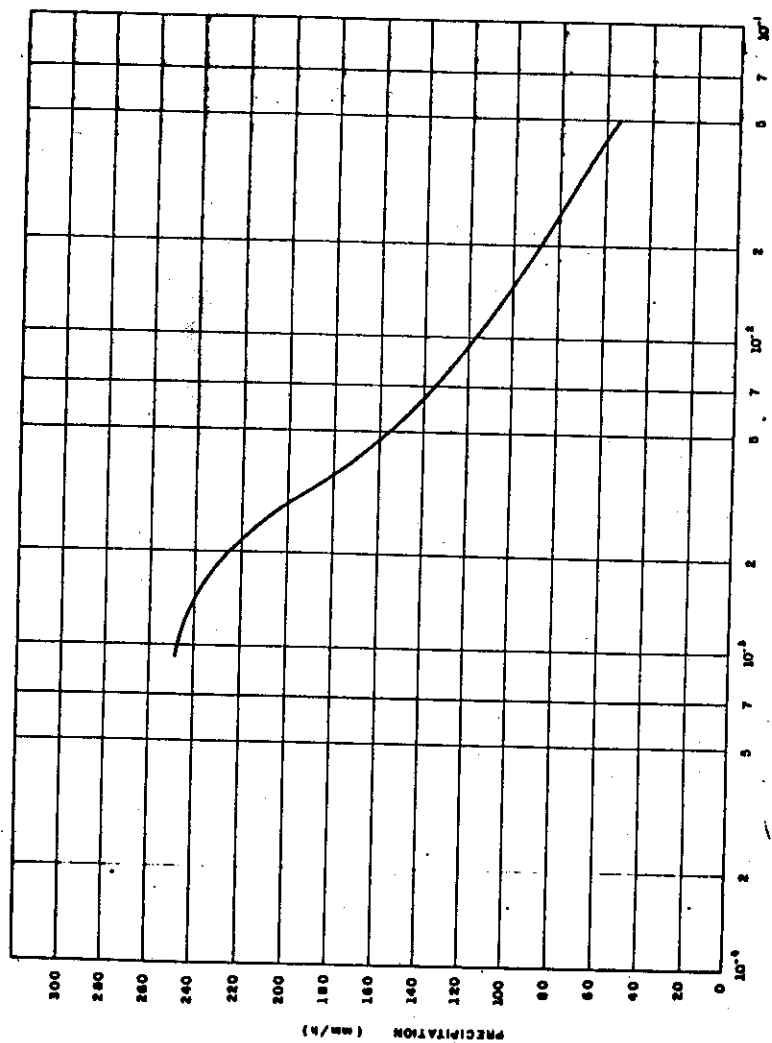


Fig. 4.8 - Statistical distribution of precipitation rate

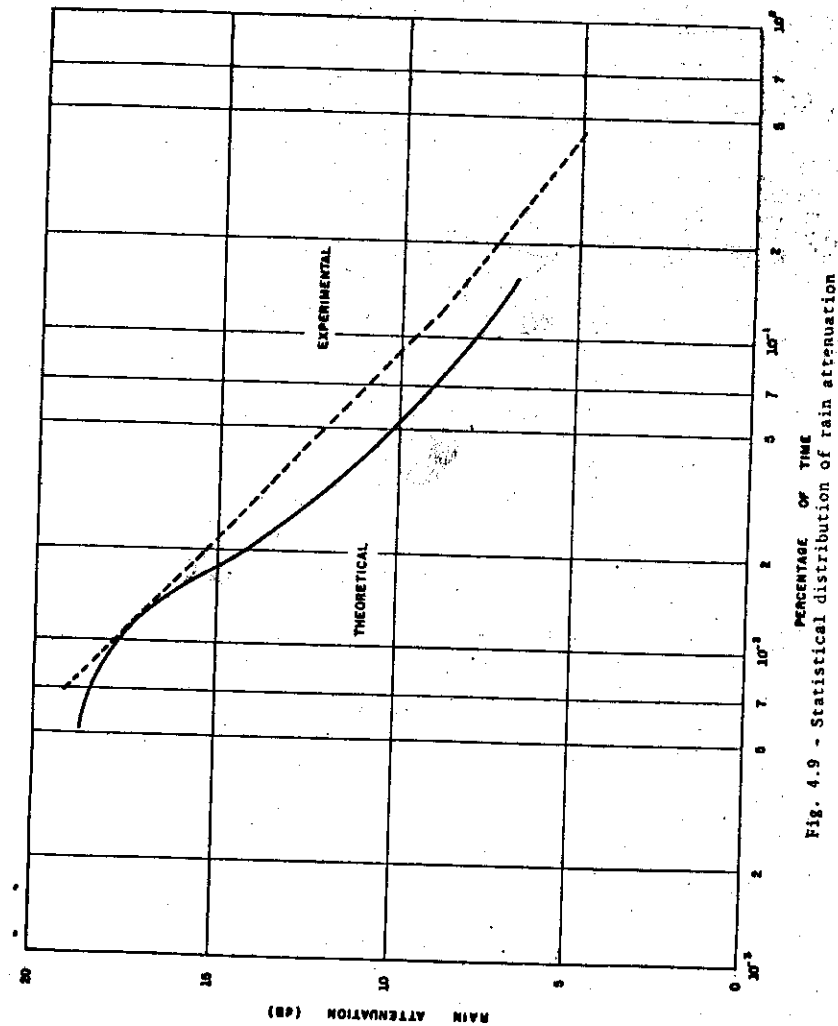


Fig. 4.9 - Statistical distribution of rain attenuation

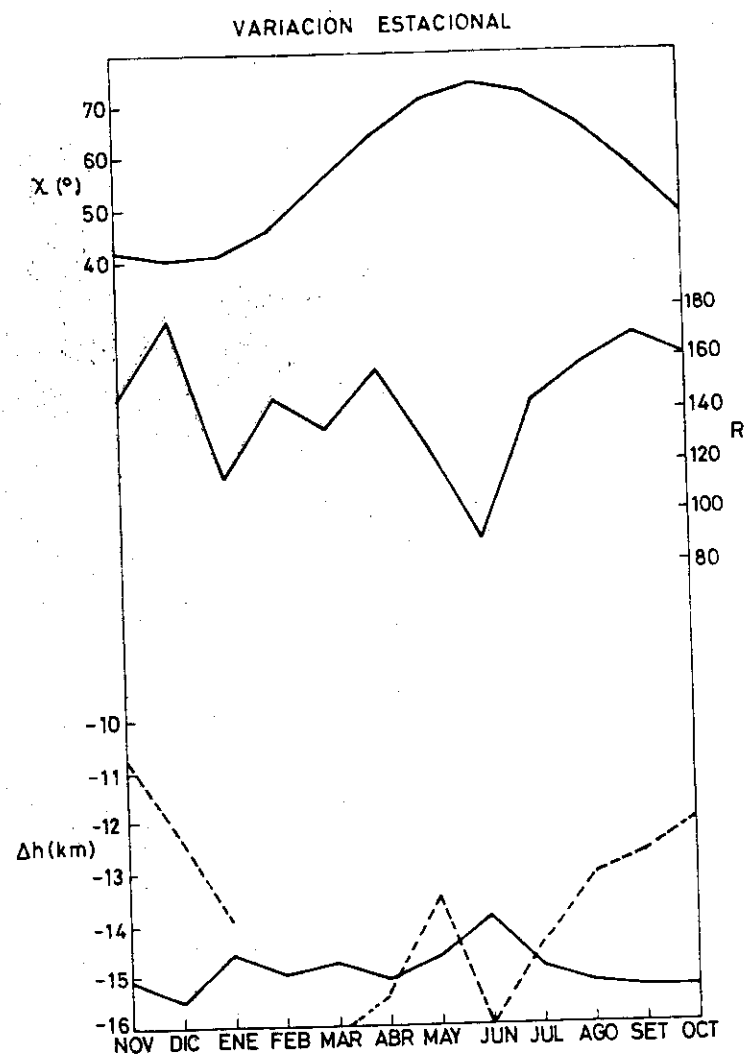


Fig. 4

21

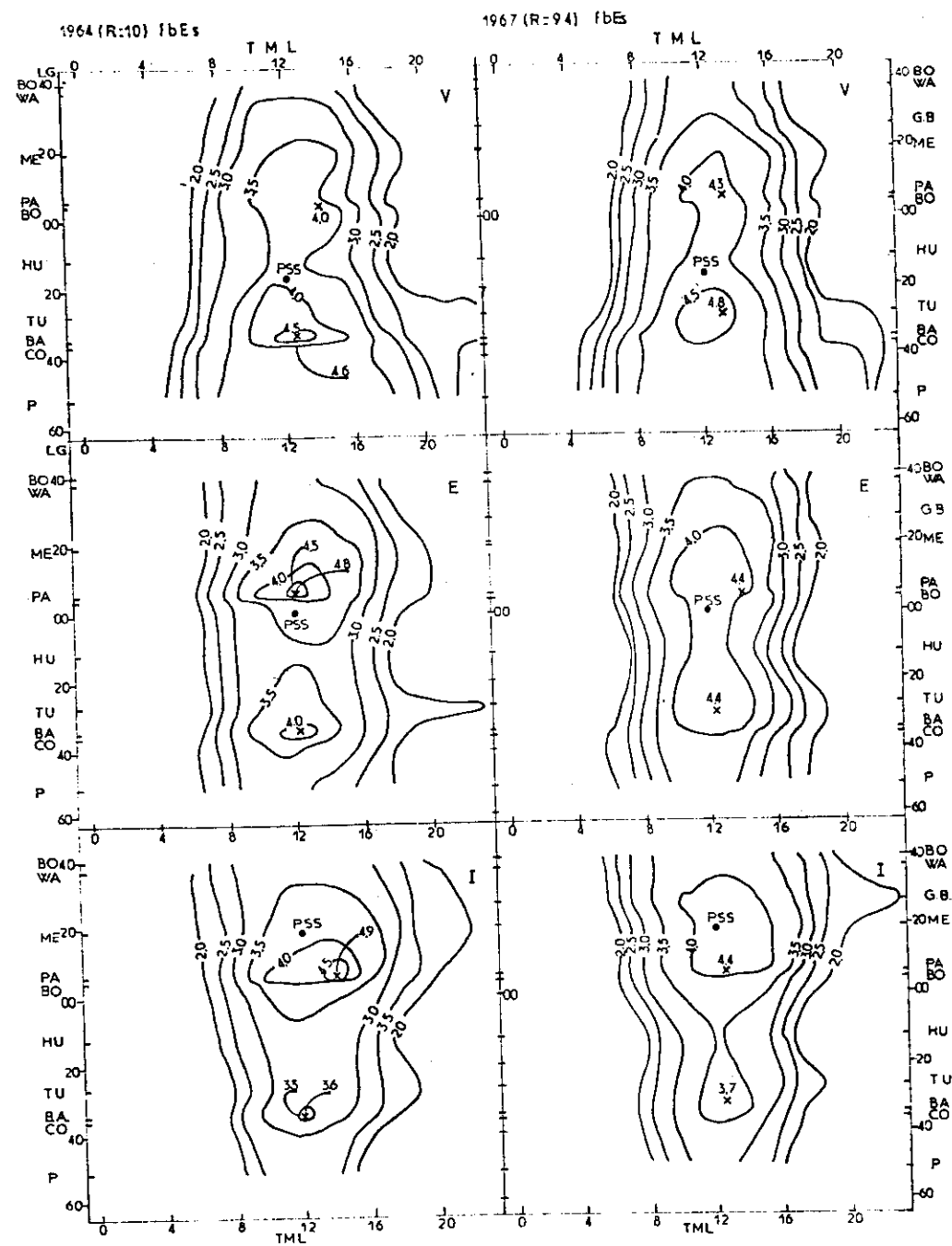


Fig. 1.22

-22-

